The Ce-Cu (Cerium-Copper) System

By P.R. Subramanian and D.E. Laughlin
Carnegie-Mellon University

Equilibrium Diagram

The equilibrium phases in the Cu-Ce system include: (1) the liquid, L, without any miscibility gaps; (2) the fcc terminal solid solution (Cu) (the maximum solid solubility of Ce in (Cu) is close to 0.1 at.% Ce); (3) the Ce-rich dcph terminal solid solution, (βCe), based on the equilibrium phase of pure Ce below 139 °C (the solid solubility of Cu in (βCe) is negligible); (4) the Ce-rich fcc terminal solid solution, (γCe), based on the equilibrium phase of pure Ce between 139 and 726 °C (the maximum solid solubility of Cu in (γCe) is ~0.37

Table 1 Solid Solubility of Ce in (Cu)

Reference	Temperature, °C	Composition, at.% Ce	Technique
[64Dui](a)	870	0.091	Metallography microhardness, and electrical resistivity
	800	0.068	
	500	0.041	
	300	0.032	
	20	0.023	
[71Kor]	850	0.100	Metallography microhardness, and electrical resistivity
	800	0.045	
	20	0.030	

(a) Compositions were obtained as wt.% from the solvus boundary given in [64Dui] and then converted to at.%.

Fig. 1 Assessed Cu-Ce Phase Diagram with Selected Experimental Data

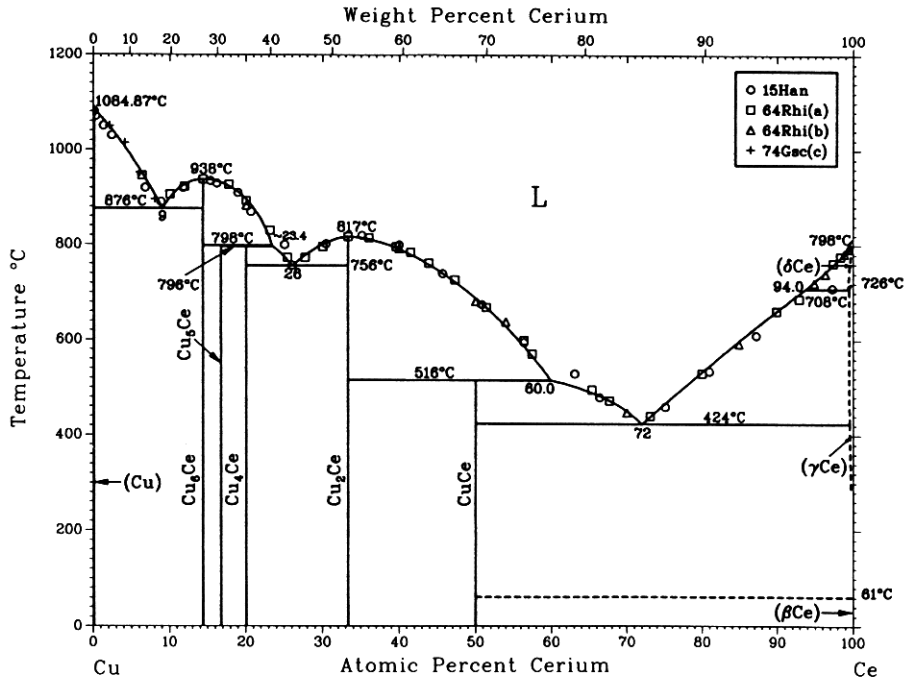

Note: Invariant temperatures have been taken from [64Rhi]. (a) Alloys made from low purity Ce. (b) Alloys made from high purity Ce. (c) Liquidus data from the Cu-rich end. P.R. Subramanian and D.E. Laughlin, 1988.

Fig. 2 Enlarged Portion of the Cerium-Rich Region of the Assessed Cu-Ce Phase Diagram with Selected Data Points

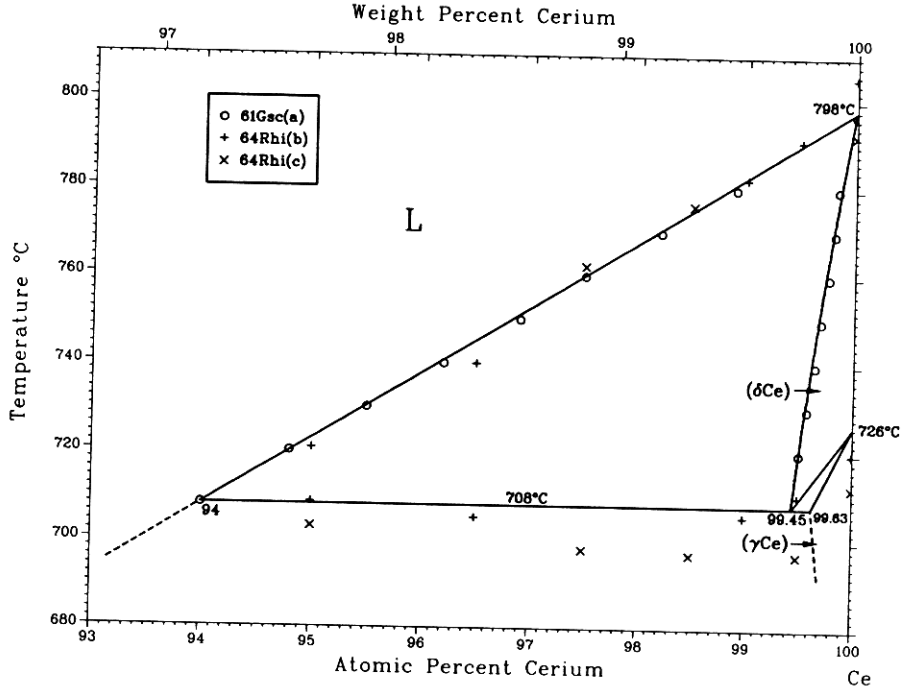

(a) Data read out from the phase diagram of [61Gsc]. (b) Experimental data from high purity Ce. (c) Experimental data from low purity Ce.
P.R. Subramanian and D.E. Laughlin, 1988.

at.% Cu at 708 °C); (5) the Ce-rich bcc terminal solid solution, (δCe), based on the equilibrium phase of pure Ce between 726 and 798 °C (the maximum solid solubility of Cu in (δCe) is ~0.55 at.% Cu at 708 °C); (6) the orthorhombic intermediate phase, Cu_6Ce, stable up to the congruent melting temperature of 938 °C; (7) the hexagonal phase, Cu_5Ce, stable up to the peritectic temperature of 798 °C; (8) the orthorhombic phase Cu_4Ce, stable up to the peritectic temperature of 796 °C; (9) the orthorhombic phase, Cu_2Ce, stable up to the congruent melting temperature of 817 °C; and (10) the equiatomic phase, CuCe, stable up to the peritectic temperature of 516 °C.

The assessed Cu-Ce equilibrium diagram shown in Fig. 1 is derived primarily from the work of [64Rhi], with the elemental melting points adjusted to conform to the accepted value for Cu from [Melt] and for Ce from [78Bea] and [86Gsc]. The diagram has been determined from thermal analysis, metallography, X-ray diffraction, and microhardness data. The original phase diagram investigation of [15Han] is in general agreement with the diagram of Fig. 1, with some variations in the reported invariant temperatures and in some instances, the eutectic compositions. In addition, [15Han] did not report the existence of Cu_5Ce. The Cu-Ce phase diagram of [61Gsc] was established primarily from an earlier report of Rhinehammer and co-workers (as quoted in [61Gsc]). Although in excellent agreement with the assessed phase diagram, the diagram of [61Gsc] also did not indicate the formation of Cu_5Ce. This phase was first reported by [61Dwi], who conducted lattice parameter studies on a large number of AB_5 compounds. Subsequently, [64Rhi] confirmed the existence of the hexagonal Cu_5Ce phase from electron microprobe X-ray analysis of metallographic samples and from single-crystal analysis. [64Rhi] suggested that the close proximity of the incongruent melting temperatures of Cu_5Ce and Cu_4Ce prevented their detection as separate phases in earlier investigations. The existence of Cu_5Ce was accepted in a subsequent revision of the Cu-Ce system by [74Gsc].

The Ce-rich end of the Cu-Ce equilibrium diagram, shown in Fig. 2, is taken from [61Gsc], with minor changes in the (γCe) ↔ (δCe) transformation temperature and in the elemental Ce melting point. At high temperatures, the Ce-rich end of the diagram is characterized by the catatectic decomposition of (δCe) at 708 °C to form (γCe) and the liquid. [64Rhi] conducted extensive investigations in this region with both high-purity Ce and lower purity Ce (the impurity content was not given). In the high-temperature Ce-rich end of the diagram of [64Rhi], the exact nature of the transformation occurring at the invariant temperature of 708 °C is not very clear. Presumably,

the transformation takes place through a catatectic reaction in concurrence with [61Gsc]. The data, however, indicate that the invariant temperature is lowered by as much as 10 °C with the use of the lower purity Ce. In addition, [64Rhi] observed a solid-state transformation at 408 °C in the region 40 to 100 at.% Ce. This transformation was, however, not observed when high-purity Ce was used. Solid-state transformations have also been reported in Ce-rich alloys by [15Han] at 368 °C and by [61Gsc] at 386 °C. An additional thermal arrest was observed by [64Rhi] at 488 °C in the region 38 to 51 at.% Ce. [64Rhi] concluded that impurities in Ce cause all of these solid-state transformations to occur, thus indicating the influence of Ce purity on the phase relations in the Cu-Ce system. Therefore, these transformations are not shown in the assessed phase diagram.

Terminal Solid Solubility

[64Dui] determined the solid solubility of Ce in Cu on the basis of metallography, microhardness, and resistivity data. They have observed a maximum solid solubility of ~0.1 at.% Ce at 870 °C. [52Bys] reported that the solid solubility of Ce in Cu is less than 0.5 at.% Ce at 770 °C, whereas [71Kor] reported a maximum solubility of 0.1 at.% Ce at 850 °C. The various results are summarized in Table 1. The maximum solid solubilities of Cu in (δCe) and (γCe) are ~0.55 and ~0.37 at.% Cu, respectively, derived from [61Gsc].

Table 2 Select Experimental Data on the Cu-Ce Liquidus Boundaries

Reference	Composition, at.% Ce	Temperature, °C
[64Rhi](a)	20	882.7
	40	792.3
	50	680.8
	54	638.5
	70	448.1
	85	592.3
	95	720.8
	96.5	740.0
	99	782.3
	99.5	791.9
	100	805.4
[64Rhi](b)	6.3	946.2
	10.0	905.8
	11.9	923.1
	14.3	938.0
	17.7	926.9
	20.0	892.3
	23.1	830.8
	25.4	773.1
	27.7	773.1
	30.0	796.2
	33.3	817.0
	36.0	815.4
	39.6	796.2
	41.5	784.6
	43.9	761.5
	47.3	726.9
	51.4	669.2
	56.4	600.0
	57.5	571.2
	65.4	496.2
	67.7	473.1
	73.1	440.4
	80.0	530.7
	90.0	661.5
	93.0	687.3
	97.5	762.3
	98.5	776.2
	100	792.3
[74Gsc](c)	0	1083.0
	2	1049.6
	4	1014.4
	6	952.0
	8	896.0
[61Gsc](d)	94.0	708
	94.8	720
	95.5	730
	96.2	740
	96.9	750
	97.5	760
	98.2	770
	98.9	780
	100	797
[15Han](e)	0	1080
	0.2	1070
	1.2	1050
	2.3	1030
	6.7	920
	8.8	890
	11.7	920
	15.3	935
	16.1	930
	18.9	910
	20.6	870
	25.0	800
	26.0	757
	30.4	802
	35.1	820
	40.0	800
	45.7	740
	50.8	675
	56.4	595
	63.1	530
	66.4	480
	75.1	460
	81.0	535
	87.3	610
	97.4	710

(a) Experimental data for alloys made with high-purity Ce. (b) Experimental data for alloys made with lower purity Ce. (c) Data for the Cu-rich end, from the phase diagram of [74Gsc]. (d) Data from the Ce-rich end of the phase diagram of [61Gsc]. (e) Liquidus compositions and temperatures taken from thermal analysis data of [15Han].

Table 3 Special Points of the Assessed Cu-Ce Phase Diagram

Reaction	Compositions of the respective phases, at.% Ce			Temperature, °C	Reaction Type	Reference
(Cu) ↔ L		0.0		1084.87	Melting point	[Melt]
L ↔ (Cu) + Cu_6Ce	8.5	~0	14.3	870	Eutectic	[15Han]
	8.5	~0	14.3	876		[61Gsc](a)
	...	~0.1	...	870 ± 5		[64Dui]
	9.0	**~0**	**14.3**	**876**		[64Rhi]
	9.0	~0	...	877		[73Hoh]
L ↔ Cu_6Ce		14.3		935	Congruent	[15Han]
		14.3		**938**		[64Rhi]
		14.3		937		[73Hoh]
L + Cu_6Ce ↔ Cu_5Ce	**23.4**	**14.3**	**16.7**	**798**	Peritectic	[64Rhi]
L + Cu_5Ce ↔ Cu_4Ce	**23.5**	**16.7**	**20.0**	**796**	Peritectic	[64Rhi]
L ↔ Cu_4Ce + Cu_2Ce	26.3	20.0	33.3	755	Eutectic	[15Han]
	26.3	20.0	33.3	756		[61Gsc](a)
	26.0	**20.0**	**33.3**	**756**		[64Rhi]
L ↔ Cu_2Ce		33.3		820	Congruent	[15Han]
		33.3		**817**		[64Rhi]
L + Cu_2Ce ↔ CuCe	62.6	33.3	50.0	515	Peritectic	[15Han]
	60.3	33.3	50.0	516		[61Gsc](a)
	60.0	**33.3**	**50.0**	**516**		[64Rhi]
L ↔ CuCe + (γCe)	72	50	~0	415	Eutectic	[15Han]
	72	**50**	**<0.5**	**424**		[64Rhi]
	72	50		422 ± 2		[65Per]
(δCe) ± (γCe) + L	**~99.5**	**~99.6**	**~94.0**	**708**	Catatectic	[61Gsc](a)
	~99.5	...	~94.2	708		[64Rhi]
(γCe) ↔ (δCe)		100		726	Allotropic	[78Bea, 86Gsc]
(δCe) ↔ L		0.0		798	Melting point	[78Bea, 86Gsc]

Note: Select values for the assessed phase diagram are shown in boldface type.
(a) Data of [61Gsc] are included only if different from the data of [64Rhi].

Liquidus and Solidus

The melting points of Cu and (δCe) are 1084.87 [Melt] and 798 °C [78Bea, 86Gsc], respectively. The experimental liquidus data from the various reports are listed in Table 2. In all instances, the temperatures shown for the experimental data are as reported and have not been corrected for the 1968 temperature scale (IPTS-68).

The initial slope of the solidus at the Ce-rich end was evaluated from the liquidus data of Fig. 3, along with the enthalpy of fusion and melting point data of (δCe). The resultant solidus slope was estimated as –169.9 °C/at.% Cu, in fairly good agreement with the solidus slope from the phase diagram of [61Gsc].

The reported compositions and temperatures of the various invariant reactions are listed in Table 3. The present evaluators have shown that the melting temperatures of the Cu-lanthanide intermediate phases show a systematic variation as one progresses across the lanthanide series. (see "The Copper-Rare Earth Systems"). In this context, the accepted melting temperatures of the various Cu-Ce intermediate phases fit in with the general trend established for the other Cu-lanthanide systems.

Three eutectic reactions occur in the Cu-Ce system. These include:

- The liquid at 9 at.% Ce, in equilibrium with (Cu) and Cu_6Ce at 876 °C. The eutectic composition and temperature are taken from [64Rhi] and are in good agreement with the data from [73Hoh]. The phase diagram of [15Han] indicated the eutectic reaction at 8.5 at.% Ce and 870 ± 5 °C.
- The liquid at 26 at.% Ce, in equilibrium with Cu_4Ce and Cu_2Ce at 756 °C. The data are taken from [64Rhi], and are in close accord with the data of [15Han].
- The liquid at 72 at.% Ce, in equilibrium with CuCe and (γCe) at 424 °C [64Rhi]. [65Per] concluded on the basis of density measurements that the most Ce-rich eutectic reaction occurs at a temperature of 422 ± 2 °C and at a composition of ~72 at.% Ce, in corroboration with the results of [64Rhi]. Although the eutectic composition reported by [15Han] is in agreement with the data of [64Rhi], their value for the eutectic temperature is 9 °C lower than the accepted value. This may be explained by impurities in the Ce metal used by [15Han]. Their Ce metal was only 96.7% pure and had a melting point of 715 °C, which is considerably lower than the currently ac-

Fig. 3 Assessed vs Calculated Cu-Ce Phase Diagram

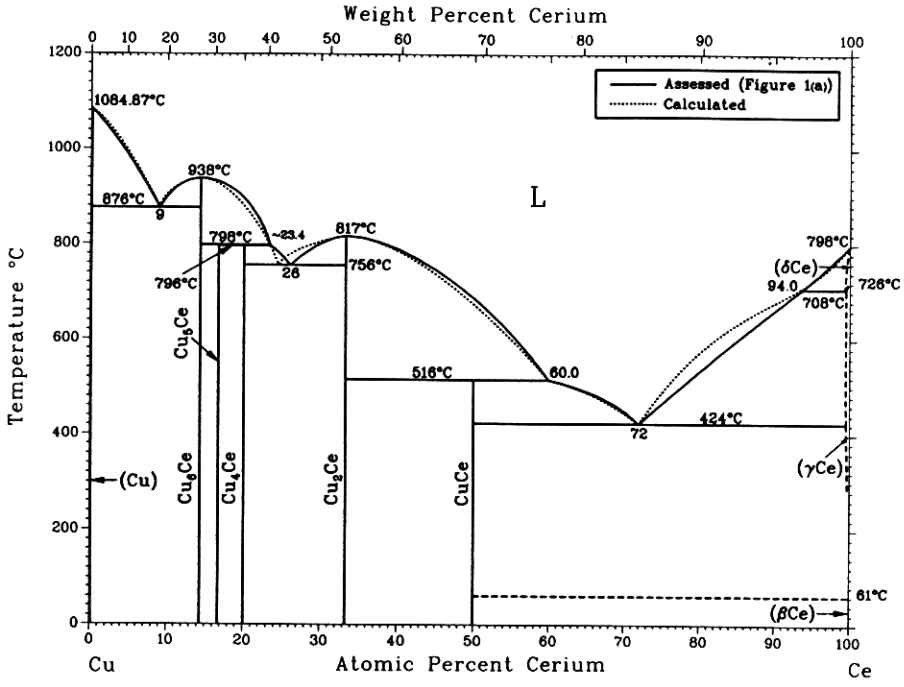

P.R. Subramanian and D.E. Laughlin, 1988.

cepted melting point of 798 °C. Therefore, the impurities in the Ce metal might have contributed to the lowering of the eutectic temperature in the Ce-rich end.

The eutectic compositions of [64Rhi], in all instances, are reported to be accurate within ±1 at.%, and the eutectic temperatures are reported to fall within ±2 °C.

Intermediate Phases

The Cu-Ce system consists of five intermediate phases, Cu_6Ce, Cu_5Ce, Cu_4Ce, Cu_2Ce, and CuCe, all of which are reported to be stoichiometric in composition.

Cu_6Ce

Cu_6Ce is formed from the liquid through a congruent transformation. The melting temperature of 938 °C is taken from [64Rhi]. The melting temperatures reported by [15Han] and by [73Hoh] are within 3 °C of the accepted melting temperature for Cu_6Ce.

Cu_5Ce

Cu_5Ce forms from Cu_6Ce and the liquid ~23.2 at.% Ce and 798 °C through a peritectic reaction. The existence of this phase was first reported by [61Dwi], and later corroborated by [64Rhi] on the basis of metallographic and single-crystal analyses. [15Han] and [61Gsc] did not observe the formation of this phase, presumably because Cu_5Ce and the adjacent phase Cu_4Ce form within a temperature interval of only 2 °C.

Cu_4Ce

Cu_4Ce forms at 796 °C by a peritectic reaction from Cu_5Ce and the liquid at ~23.4 at.% Ce. In the report of [61Gsc], this phase was assigned the stoichiometry $Cu_{4.8}Ce_{1.2}$ with a structure similar to that of Cu_5Ca. However, in a subsequent compilation by [74Gsc], the existence of Cu_4Ce as a separate compound was accepted along with the existence of Cu_5Ce.

$Cu_{3.6}Ce$

$Cu_{3.6}Ce$, with a stoichiometry very close to that of Cu_4Ce, was observed by [84All]. According to results from an earlier unpublished work by the same author (as quoted in [84All]), the $Cu_{3.6}Ce$ phase exists over a narrow temperature range, and that its formation cannot be observed during solidification at normal cooling rates. Apparently, $Cu_{3.6}Ce$ is a metastable phase and forms only under rapid cooling. As such, its occurrence is not shown in the assessed equilibrium diagram.

Cu_2Ce

Cu_2Ce forms congruently at 817 °C. The accepted melting temperature from [64Rhi] is 3 °C lower than the value reported by [15Han].

CuCe

CuCe, the equiatomic phase, is the most Ce-rich intermediate phase, and forms from Cu_2Ce and the liquid

Table 4 Cu-Ce Experimental Lattice Parameter Data

Phase	Crystal structure	Lattice parameters, nm a	b	c	Reference
Cu_6Ce	Orthorhombic	0.8085	0.5097	1.0172	[52Bys]
		0.8112 ± 0.0001	0.5102 ± 0.0001	1.0162 ± 0.0001	[60Cro]
		0.8108	0.5102	1.0160	[70Bus]
Cu_5Ce	Hexagonal	0.5141	...	0.4132	[48Heu](a)
		0.5150 ± 0.0002	...	0.4102 ± 0.0002	[52Bys](a)
		0.5146	...	0.4108	[61Dwi]
		0.514 ± 0.001	...	0.411 ± 0.001	[64Rhi]
		0.5149	...	0.4108	[71Bus](b)
Cu_4Ce	Orthorhombic	0.454 ± 0.001	0.810 ± 0.001	0.919 ± 0.001	[64Rhi]
$Cu_{3.6}Ce$	Hexagonal	1.1858 ± 0.0004	... ...	0.9107 ± 0.0003	[84All]
Cu_2Ce	Orthorhombic	0.443 ± 0.001	0.705 ± 0.002	0.745 ± 0.002	[61Lar1]
		0.4425 ± 0.0005	0.7057 ± 0.0005	0.7475 ± 0.0005	[63Sto](c)
		0.4433	0.7064	0.7472	[77Olc](d)
CuCe	Orthorhombic	0.730 ± 0.002	0.430 ± 0.002	0.636 ± 0.002	[61Lar2]
		0.719	0.430	0.623	[65Wal]
		0.7370	0.4623	0.5648	[65Dwi](e)

(a) Data quoted for Cu_4Ce. (b) Alloys made from 99.99% pure Cu and 99.9% pure Ce. (c) Alloys made from 99.999% pure Cu and 99+% pure Ce. (d) Alloys made from 99.999% pure Cu and 99.9% pure Ce. (e) As quoted in [74Gsc].

Table 5 Cu-Ce Crystal Structure Data

Phase	Composition range, at.% Ce	Pearson symbol	Space group	Strukturbericht designation	Prototype
(Cu)	0	*cF4*	$Fm\bar{3}m$	*A1*	Cu
Cu_6Ce	~14.29	*oP28*	*Pnma*	...	$CeCu_6$
Cu_5Ce	~16.67	*hP6*	*P6/mmm*	$D2_d$	$CaCu_5$
Cu_4Ce	~20.0	*oP20*	*Pnnm*	...	$CeCu_4$
Cu_2Ce	~33.3	*oI12*	*Imma*	...	$CeCu_2$
CuCe	~50	*oP8*	*Pnma*	*B27*	FeB
(δCe)	100	*cI2*	$Im\bar{3}m$	*A2*	W
(γCe)	100	*cF4*	$Fm\bar{3}m$	*A1*	Cu
(βCe)	100	*hP2*	$P6_3/mmc$	*A3*	Mg
(αCe)	100	*cF4*	$Fm\bar{3}m$	*A1*	Cu

of composition ~60 at.% Ce through a peritectic transformation. The reaction temperature of 516 °C is taken from [64Rhi], and is in good agreement with that of [15Han].

Crystal Structures and Lattice Parameters

The reported lattice parameter values for the various Cu-Ce intermediate phases are given in Table 4.

The Cu_6Ce phase was first investigated by [52Bys], who concluded from single-crystal analyses that Cu_6Ce is orthorhombic. Their investigations were conducted on alloys made from 99.99% pure Cu and ~98.5% pure Ce. [60Cro] carried out a detailed structural investigation of Cu_6Ce and concluded that the Cu_6Ce structure can be considered as a new prototype. Phases with the Cu_6Ce stoichiometry and prototype structure have been observed to form in a number of Cu-lanthanide systems (see "The Copper-Rare Earth Systems," in this issue). The Cu_6Ce phase also was investigated by [70Bus]. Their lattice parameter data for Cu_6Ce are in close accord with the data of [60Cro].

[61Dwi] indicated that Cu_5Ce has a hexagonal $CaCu_5$ prototype structure. Lattice parameter data reported for this phase by [64Rhi] and [71Bus] are in good agreement with the results of [61Dwi].

Both [48Heu] and [52Bys] reported lattice parameter values for Cu_4Ce based on a hexagonal lattice. However, [64Rhi] pointed out that the data of [48Heu]

Table 6 Cu-Ce Lattice Parameter Data

Phase	Composition, at.% Ce	Lattice parameters, nm a	b	c	Comment	Reference
(Cu)	0	0.36146	...	...	At 25 °C	[Massalski]
Cu_6Ce	~14.29	0.8110	0.5102	1.0161	...	[60Cro, 70Bus]
Cu_5Ce	~16.67	0.5148	...	0.4108	...	[61Dwi, 71Bus]
Cu_4Ce	~20.0	0.458	0.810	0.935	...	(a)
Cu_2Ce	~33.3	0.4429	0.7061	0.7474	...	[63Sto, 77Olc]
CuCe	~50	0.7370	0.4623	0.5648	...	[65Dwi]
(δCe)	100	0.412	...	...	At 757 °C	[78Bea, 86Gsc]
(γCe)	100	0.51610	...	...	At 24 °C	[78Bea, 86Gsc]
(βCe)	100	0.36810	...	1.1857	At 24 °C	[78Bea, 86Gsc]
(αCe)	100	0.485	...	...	At −196 °C	[78Bea, 86Gsc]

(a) Based on [64Rhi]; the *a* and *c* parameters have been increased by 0.004 and 0.016 nm, respectively, to conform to the systematics of crystallographic data for the Cu-lanthanide systems [83Gsc, 86Sub].

Table 7 Heat Capacity Data for Liquid Cu-Ce Alloys

Composition, at.% Ce	Specific heat J/mol·K	Temperature range, °C
0	30.21 ± 0.39	1142 to 1775
19.95	32.99 ± 0.61	1386 to 1928
30.27	35.77 ± 1.46	1382 to 1819
40.70	35.24 ± 0.72	1147 to 1815
50.09	33.25 ± 1.33	1417 to 1933
61.28	32.67 ± 1.28	1410 to 1927
71.27	32.41 ± 1.57	1371 to 1945
80.24	32.43 ± 0.83	1332 to 1998
89.64	32.66 ± 0.69	1430 to 1974
100	33.36 ± 0.46	1258 to 2134

From [80Dok].

Table 8 Cu-CeThermodynamic Properties

Lattice stability parameters for Cu(a)

$G^0(Cu, L) = 0$

$G^0(Cu, fcc) = -13\,054 + 9.613\,T$

Lattice stabililty parameters for Ce(b)

$G^0(Ce, L) = 0$

$G^0(Ce, bcc) = -5460 + 5.098\,T$

$G^0(Ce, fcc) = -8450 + 8.091\,T$

Gibbs energies(c)

$G(L) = X(1-X)(-91\,328 + 55\,390\,X) + RT[X \ln X + (1-X) \ln (1-X)]$

$\Delta_f G(Cu_6Ce) = -20\,298 + 4.91\,T$

$\Delta_f G(Cu_5Ce) = -20\,480 + 4.00\,T$

$\Delta_f G(Cu_4Ce) = -16\,394 + 0.99\,T$

$\Delta_f G(Cu_2Ce) = -35\,949 + 13.03\,T$

$\Delta_f G(CuCe) \doteq -32\,559 + 14.50\,T$

Note: Standard states: pure liquid Cu and pure liquid Ce. Gibbs energies are expressed in J/mol, and temperatures are in K. *X* is the atomic fraction of Ce. Mol refers to the atom as the elementary entity.

(a) From [Hultgren,E]. (b) From [83Cha]; melting and transformation temperatures are from [78Bea] and [86Gsc]. (c) From the phase diagram [this work].

and [52Bys] might actually refer to Cu_5Ce, because their reported density and lattice parameter values for Cu_4Ce correspond closely with the calculated values for Cu_5Ce. Preliminary results by [64Rhi] indicate that Cu_4Ce is orthorhombic with a probable space group *Pnnm*.

[84All] established the existence of $Cu_{3.6}Ce$ and reported that this phase crystallizes with a stoichiometry of $Cu_{51}Ce_{14}$ and with the $Ag_{51}Gd_{14}$ prototype structure. The existence of this phase was not reported by earlier researchers.

From detailed structural investigations on single crystals, [61Lar1] concluded that Cu_2Ce is orthorhombic and crystallizes with a new prototype structure. Their lattice parameter data are included in Table 4, along with the reported lattice parameter values of [63Sto] and [77Olc]. The accepted lattice parameters are based on [77Olc]; the data of [61Lar1] were not used because the "*c*" parameter value reported by these authors does not agree with the results of other investigators.

The lattice parameters reported by [61Lar2], [65Dwi], and [65Wal] for CuCe disagree with one another. In this context, [74Gsc] accepted the set of lattice parameter values reported by [65Dwi] as the most accurate, based on the critical analysis of [66Hoh] on ~40 FeB, *B*27-type structures. The present authors were unable to resolve the discrepancy in the reported lattice parameter data; however, the lattice parameter values of [65Dwi] are consistent with the systematic decrease in lattice parameters with increasing atomic number. Accordingly, the accepted lattice parameter data for CuCe are from [65Dwi], in concurrence with the judgment of [74Gsc].

The accepted lattice parameter data, crystal structures, and related parameters for the various phases are shown in Tables 5 and 6. Also included are the corresponding data for (Cu), as well as for the various polymorphs of Ce.

Table 9 Calculated Enthalpies of Formation of Cu-Ce Intermediate Phases vs Theoretical Estimates Based on Miedema's Model

Phase	Enthalpy of formation, kJ/mol Present modeling	Miedema model(a)
Cu_6Ce	-20.3	-28.4
Cu_5Ce	-20.5	-30.8
Cu_4Ce	-16.4	-34.0
Cu_2Ce	-36.0	-42.4
CuCe	-32.6	-40.9

Note: Standard states are liquid Cu and liquid Ce.
(a) From [83Nie].

Thermodynamics

Thermodynamic Measurements

No experimental thermodynamic data are available for the solid Cu-Ce alloys, although heat capacity data have been reported for liquid Cu-Ce alloys over the complete range of alloy compositions [80Dok]. Their heat capacity results are shown in Table 7. Also, [80Dok] expressed the heat capacity of the liquid Cu-Ce alloys as:

$$C_p = 4.22 + 29.08\exp(-0.108X_{Cu}) + 4.99\exp[-36.44(X_{Cu} - 0.67)^2 \text{ J/mol·K} \quad \text{(Eq 1)}$$

where X_{Cu} is the mole fraction of Cu. Moreover, [80Dok] observed that the composition variation of the heat capacity shows a maxima corresponding to the stoichiometry of the intermediate phase Cu_2Ce. They interpreted this maxima as being due to atomic clustering in the liquid Cu-Ce alloys, thereby resulting in the structure of Cu_2Ce being retained in the liquid state.

Thermodynamic Modeling

The Cu-Ce liquidus boundaries are fairly well-established, and therefore can be used to derive expressions for the thermodynamic functions of the liquid, as well as for the intermediate phases. The thermodynamic functions can then be used to calculate the various phase boundaries for comparison with the experimental data. In the present evaluation, the following assumptions were made:

- The solid phases (Cu), (δCe), and (γCe) have no significant solid solubility.
- The lattice stability parameters for the (Cu) and (δCe) phases are derived from the enthalpies of fusion, as well as the melting points of the respective elements. The lattice stability parameters for (γCe) are derived from those for (δCe) as well as the temperature and enthalpy of the allotropic transformation (γCe) ↔ (δCe). The resultant expressions are given in Table 8, where pure liquid Cu and pure liquid Ce have been chosen as standard states.
- The liquid behaves like a subregular solution. The integral molar excess Gibbs energy for the liquid can, therefore, be expressed in terms of two temperature-independent parameters as follows:

$$G^{ex}(L) = X(1-X)(A + BX) \quad \text{(Eq 2)}$$

where X is the atomic fraction of Ce.

All of the intermediate phases are line phases, i.e., the phases show nil homogeneity ranges.

In the present evaluation, data for the two eutectic points at 9 at.% Ce, 876 °C and 72 at.% Ce, 424 °C were utilized to derive the integral molar excess Gibbs energy of the liquid. The resultant expression for the integral Gibbs energy of the liquid is given in Table 8.

The integral molar Gibbs energies of the intermediate phases were next derived from consideration of equilibrium between the liquid and the respective intermediate phases at various invariant temperatures. The Gibbs energies of the phases at various temperatures were then fitted by least-squares analysis to give the expressions that are listed in Table 8. For Cu_6Ce and Cu_2Ce, the Gibbs energy functions were determined from liquid data at three different temperatures: 938, 876 and 798 °C for Cu_6Ce and 817, 756, and 516 °C for Cu_2Ce, respectively.

The liquidus boundaries were calculated at selected temperatures from the thermodynamic functions listed in Table 8. The calculated liquidus is compared with the experimental phase boundaries in Fig. 3. The calculated phase boundaries match quite well with the experimental liquidus, with some exceptions in selected regions. The calculated eutectic composition at 756 °C lies at 24.7 at.% Ce, and is accompanied by shifts of the L + Cu_4Ce/L liquidus and the L/L + Cu_2Ce liquidus towards higher Cu content. These liquidus boundaries were determined as follows: the L/L + Cu_2Ce boundary and the eutectic composition at 756 °C were first established by considering equilibrium of the liquid with the Cu_2Ce phase. The molar Gibbs energy of the Cu_4Ce phase was next evaluated from data at 796 and 756 °C, corresponding to liquid compositions 23.5 at.% Ce and 24.7 at.% Ce, respectively. The resultant expression for the Gibbs energy of Cu_4Ce was then utilized to calculate the L + Cu_4Ce/L liquidus.

In order to observe if any improvements could be made in this region, the stability parameters for Cu_2Ce were re-evaluated by selecting liquidus data at only two of the three reported invariant temperatures at any instance. The resultant expressions for the Gibbs energy of Cu_2Ce are as follows:

$$\Delta_f G(756 \text{ and } 817\ ^\circ\text{C}) = -27\,667 + 5.24\,T \text{ (J/mol)} \quad \text{(Eq 3)}$$

$$\Delta_f G(516 \text{ and } 817\ ^\circ\text{C}) = -35\,591 + 12.51\,T \text{ (J/mol)} \quad \text{(Eq 4)}$$

$$\Delta_f G(516 \text{ and } 756\ ^\circ\text{C}) = -37\,048 + 14.36\,T \text{ (J/mol)} \quad \text{(Eq 5)}$$

The temperatures in parentheses refer to the two invariant temperatures that were used for evaluating the Gibbs energy expressions. The calculated L + Cu_2Ce/L liquidus between 817 and 516 °C from Eqs 4 and 5 agreed well with the experimental liquidus, whereas the L/L + Cu_2Ce liquidus between 756 and 817 °C and to the left of the congruent melting temperature of 817 °C was quite inconsistent with the experimental liquidus. The expression from Eq 3 showed good results for the L/L + Cu_2Ce liquidus to the left of the congruent temperature. However, the L + Cu_2Ce/L liquidus between 817 and 516 °C showed deviation from the experimental liquidus toward higher Cu content. As such, the Gibbs energy expression for Cu_2Ce shown in Table 8 was deemed most reliable and most consistent with the experimental liquidus.

The decomposition temperatures of the various intermediate phases were determined from the temperature variation of the molar Gibbs energies of the phases. In all cases, the decomposition temperatures were found to be above their respective formation temperatures, indicating that these phases are quite stable at all points below their formation temperatures.

The enthalpies of formation obtained from the present modeling are compared in Table 9 with those derived on the basis of the semi-empirical model of Miedema [80Mie, 83Nie]. In all instances, the Miedema values are more exothermic than those obtained in the present calculation.

Cited References

15Han: F. Hanaman, "On Cerium Alloys," *Int. Z. Metallogr., 7,* 174-224 (1915) in German. (Equi Diagram; Experimental; #)

48Heu: T. Heumann, "Contribution to the Identity of A_5B Phases," *Nachr. Akad. Wiss. Goettingen, Math. Physik. Klasse, 1,* 21-26 (1948) in German. (Crys Structure; Experimental)

52Bys: A. Bystrom, P. Kierkegaard, and O. Knop, "X-Ray Investigation of Cu-Ce Alloys Rich in Copper. With a Discussion of the Interatomic Distances in the A-[5]B Structure Type," *Acta Chem. Scand., 6,* 709-715 (1952). (Equi Diagram, Crys Structure; Experimental)

60Cro: D.T. Cromer, A.C. Larson, and R.B. Roof, Jr., "The Crystal Structure of $CeCu_6$," *Acta Crystallogr., 13,* 913-918 (1960). (Crys Structure; Experimental)

61Dwi: A.E. Dwight, "Factors Controlling the Occurrence of Laves Phases and AB_5 Compounds among Transition Elements," *Trans. ASM, 53,* 479-500 (1961). (Crys Structure; Experimental)

***61Gsc:** K.A. Gschneidner, Jr., *Rare Earth Alloys,* D. Van Nostrand Co., Inc., Princeton, NJ (1961). (Equi Diagram, Crys Structure; Compilation; #)

61Lar1: A.C. Larson and D.T. Cromer, "The Crystal Structure of $CeCu_2$," *Acta Crystallogr., 14,* 73-74 (1961). (Crys Structure; Experimental)

61Lar2: A.C. Larson and D.T. Cromer, "The Crystal Structure of CeCu," *Acta Crystallogr., 14,* 545-546 (1971). (Crys Structure; Experimental)

63Sto: A.R. Storm and K.E. Benson, "Lanthanide-Copper Intermetallic Compounds having the $CeCu_2$ and AlB_2 Structure," *Acta Crystallogr., 16,* 701-702 (1963). (Crys Structure; Experimental)

64Dui: U.K. Duisemaliev and A.A. Presnyakov, "Solubility of Cerium in Copper and Physico-Mechanical Properties of Copper-Cerium Alloys," *Zhur. Neog. Khim., 9,* 2258-2260 (1964) in Russian; TR: *Russ. J. Inorg. Chem., 9*(9), 1220-1222 (1964). (Equi Diagram; Experimental)

***64Rhi:** T.B. Rhinehammer, D.E. Etter, J.E. Selle, and P.A. Tucker, "The Cerium-Copper System," *Trans. Met. Soc. AIME, 230,* 1193-1198 (1964). (Equi Diagram, Crys Structure; Experimental; #)

65Dwi: A.E. Dwight, R.A. Conner, Jr., and J.W. Downey, "Crystal Structures of Compounds of the Rare Earths with Cu, Ag, Au, and Ga," Proc. 5th Rare Earth Res. Conf., Aug 30-Sept 1, Ames, IA, *5,* 35-44 (1965). (Crys Structure; Experimental)

65Per: R.H. Perkins, L.A. Geoffrion, and J.C. Biery, "Densities of Some Low-Melting Cerium Alloys," *Trans. Met. Soc. AIME, 233,* 1703-1710 (1965). (Equi Diagram; Experimental)

65Wal: R.E. Walline and W.E. Wallace, "Magnetic and Structural Characteristics of Lanthanide-Copper Compounds," *J. Chem. Phys., 42*(2), 604-607 (1965). (Crys Structure; Experimental)

66Hoh: D. Hohnke and E. Parthe, "AB Compounds with Sc, Y, and Rare Earth Metals. II," *Acta Crystallogr., 20,* 572-582 (1966). (Crys Structure; Review)

70Bus: K.H.J. Buschow and A.S. van der Goot, "The Crystal Structure of Some Copper Compounds of the Type RCu_6," *J. Less-Common Met., 20,* 309-313 (1970). (Crys Structure; Experimental)

71Bus: K.H.J. Buschow and A.S. van der Goot, "Composition and Crystal Structure of Hexagonal Cu-Rich Rare Earth-Copper Compounds," *Acta Crystallogr. B, 27*(6) 1085-1088 (1971). (Crys Structure; Experimental)

71Kor: A.M. Korolkov and E.V. Lysova, "Solubility of Cerium and Zirconium in Copper in the Solid State," *Strukt. Svoistva Legk. Splavov,* A.M. Korolkov, Ed., Nauka, Moscow, 17-20 (1971) in Russian. (Equi Diagram; Experimental)

73Hoh: B. Hohn and A.J. Perry, "Unidirectional Growth of Copper-Cu_6Ce and Copper-Cu_6La Eutectics," *J. Inst. Met., 101,* 62-64 (1973). (Equi Diagram; Experimental)

74Gsc: K.A. Gschneidner, Jr. and M.E. Verkade, *Selected Cerium Phase Diagrams,* Report IS-RIC-7, Rare-Earth Information Center, Energy and Mineral Resources Research Institute, Iowa State University, Ames, IA, 18-19 (1974). (Equi Diagram, Crys Structure; Compilation; #)

77Olc: G.L. Olcese, "Structural and Magnetic Properties of $Ce(Cu,Ni)_2$ Pseudobinary Phases," *J. Phys. Chem. Solids, 38,* 1239-1241 (1977). (Crys Structure; Experimental)

78Bea: B.J. Beaudry and K.A. Gschneidner, Jr., "Prepara-

tion and Basic Properties of the Rare-Earth Metals," in *Handbook on the Physics and Chemistry of Rare Earths*, Vol. 1--*Metals*, K.A. Gschneidner and L. Eyring, Ed., North-Holland Physics Publishing Co., Amsterdam, 173-232 (1978). (Equi Diagram, Crys Structure; Compilation)

80Dok: W. Dokko and R.G. Bautista, "The High Temperature Heat Content and Heat Capacity of Liquid Cerium-Copper Alloys by Levitation Calorimetry," *Metall. Trans. B, 11*, 511-518 (1980). (Thermo; Experimental)

80Mie: A.R. Miedema, P.F. de Chatel, and F.R. de Boer, "Cohesion in Alloys--Fundamentals of a Semi-Empirical Method," *Physica B, 100*, 1-28 (1980). (Thermo; Theory)

83Cha: M.W. Chase, "Heats of Transition of the Elements," *Bull. Alloy Phase Diagrams, 4*(1), 123-124 (1983). (Thermo; Compilation)

83Gsc: K.A. Gschneidner, Jr. and F.W. Calderwood, "Use of Systematics for the Evaluation of Rare-Earth Phase Diagrams and Crystallographic Data," *Bull. Alloy Phase Diagrams, 4*(2), 129-131 (1983). (Equi Diagram, Crys Structure; Review)

83Nie: A.K. Niessen, F.R. de Boer, R. Boom, P.F. de Chatel, W.C.M. Mattens, and A.R. Miedema, "Model Predictions for the Enthalpy of Formation of Transition Metal Alloys II," *Calphad, 7*(1), 51-70 (1983). (Thermo; Theory)

84All: C. Allibert, W. Wong-Ng, and S.C. Nyburg, "$CeCu_{3.6}$, a Disordered Variant of $Gd_{14}Ag_{51}$ Type," *Acta Crystallogr. C, 40*, 211-214 (1984). (Crys Structure; Experimental)

86Gsc: K.A. Gschneidner, Jr. and F.W. Calderwood, "Intra Rare Earth Binary Alloys: Phase Relationships, Lattice Parameters and Systematics," in *Handbook on the Physics and Chemistry of Rare Earths*, Vol. 8, K.A. Gschneidner, Jr. and L. Eyring, Eds., North-Holland Physics Publishing Co., Amsterdam, 1-161 (1986). (Equi Diagram, Crys Structure; Compilation)

86Sub: P.R. Subramanian and D.E. Laughlin, "The Copper-Rare Earth Systems," *Bull. Alloy Phase Diagrams*, in this issue (1988). (Equi Diagram, Crys Structure; Review)

*Indicates key paper.

#Indicates presence of a phase diagram.

Cu-Ce evaluation contributed by **P.R. Subramanian,** Materials Science Division, Universal Energy Systems, Incorporated, 4401 Dayton-Xenia Road, Dayton, OH 45435 and **D.E. Laughlin,** Department of Metallurgical Engineering and Materials Science, Carnegie Mellon University, Pittsburgh, PA, 15213. Work was supported by the International Copper Research Association, Inc. (INCRA) and the Department of Energy through the Joint Program on Critical Compilation of Physical and Chemical Data coordinated through the Office of Standard Reference Data, National Bureau of Standards. The authors wish to thank Dr. K.A. Gschneidner, Jr., Director, and F.W. Calderwood, Rare-earth Information Center, Ames Laboratory, Iowa State University, Ames, IA, for providing part of the bibliographic search and the computer program for the critical evaluation of crystallographic data. The authors would also like to thank Dr. D.J. Chakrabarti for his assistance with some of the computer programs, and Dr. H. Okamoto for valuable suggestions. Literature searched through 1985. Professor Laughlin is the ASM/NBS Data Program Category Editor for binary copper alloys.

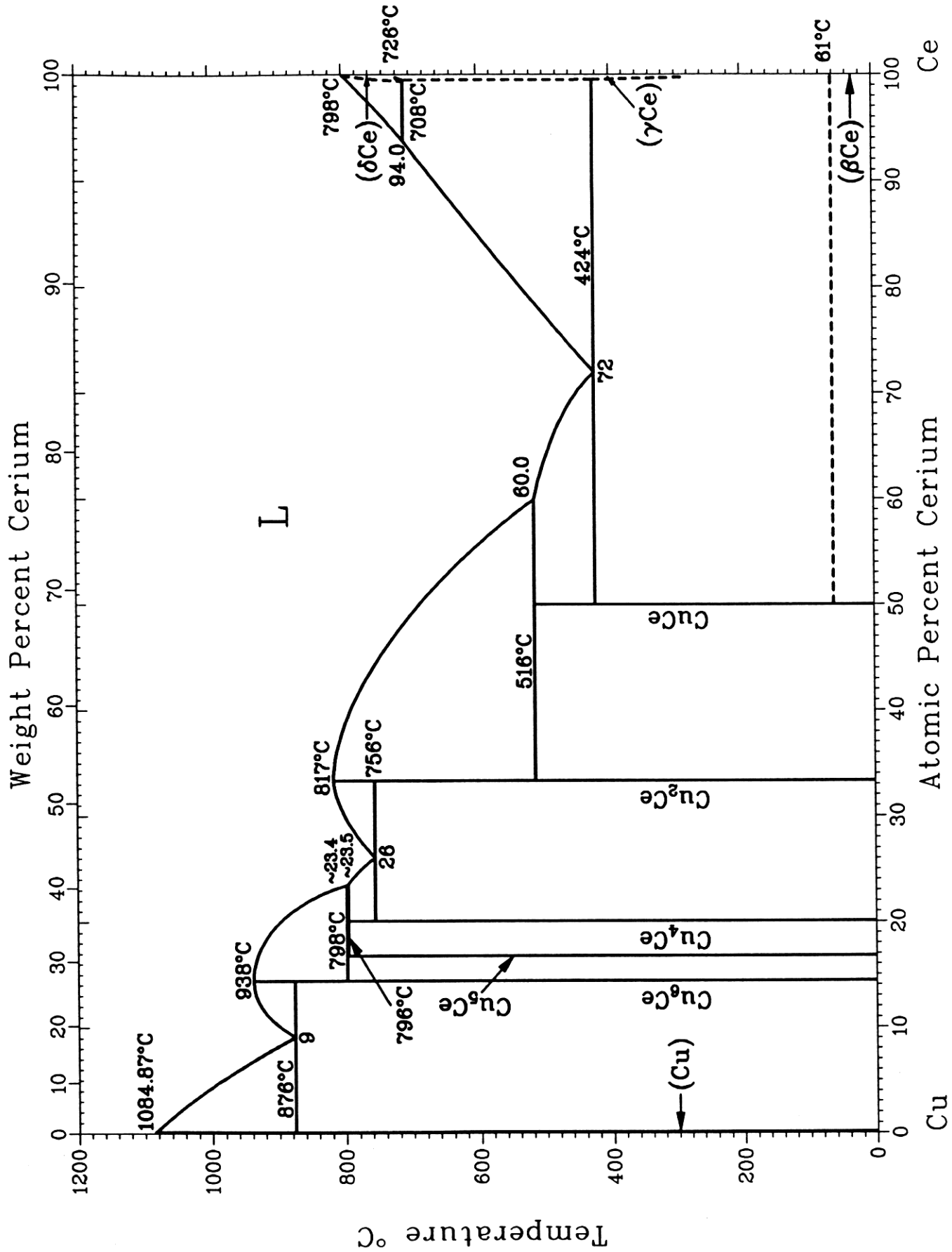

P.R. Subramanian and D.E. Laughlin

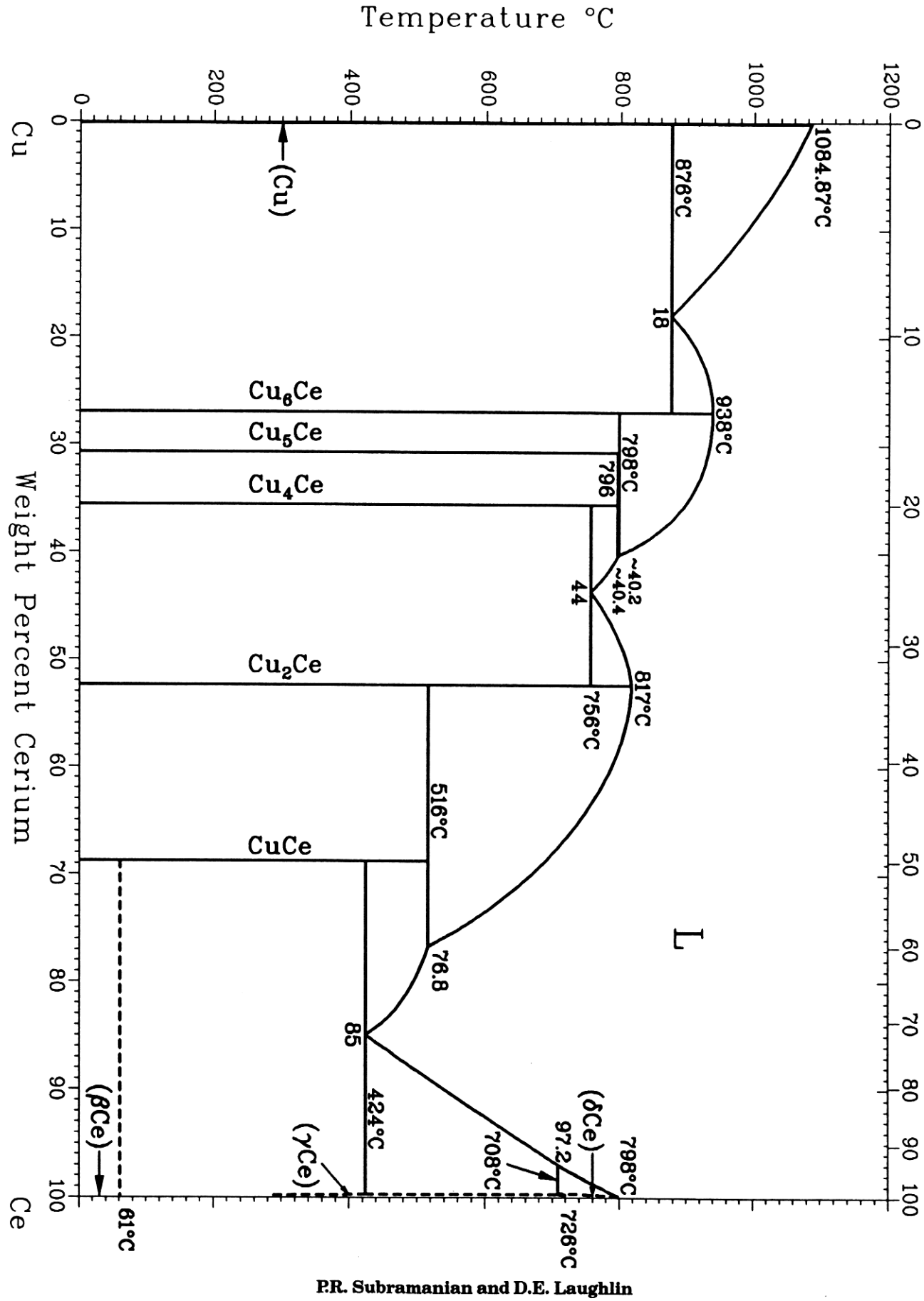

P.R. Subramanian and D.E. Laughlin